Graphene-Based Aptamer Logic Gates and Their Application to Multiplex Detection

Li Wang, Jinbo Zhu, Lei Han, Lihua Jin, Chengzhou Zhu, Erkang Wang,* and Shaojun Dong*

State Key Laboratory of Electroanalytical Chemistry, Changchun Institute of Applied Chemistry, Chinese Academy of Sciences, Changchun, Jilin 130022, China

ABSTRACT In this work, a GO/aptamer system was constructed to create multiplex logic operations and enable sensing of multiplex targets. 6-Carboxyfluorescein (FAM)-labeled adenosine triphosphate binding aptamer (ABA) and FAM-labeled thrombin binding aptamer (TBA) were first adsorbed onto graphene oxide (GO) to form a GO/aptamer complex, leading to the quenching of the fluorescence of FAM. We demonstrated that the unique GO/aptamer interaction and the specific aptamer–target recognition in the target/GO/aptamer system were programmable and could be utilized to regulate the fluorescence of FAM *via* OR and INHIBIT logic gates. The fluorescence changed according to different input combinations, and the integration of OR and INHIBIT logic gates provided an interesting approach for logic sensing applications where multiple target molecules were present. High-throughput fluorescence imagings that enabled the simultaneous processing of many samples by using the combinatorial logic gates were realized. The developed logic gates may find applications in further development of DNA circuits and advanced sensors for the identification of multiple targets in complex chemical environments.

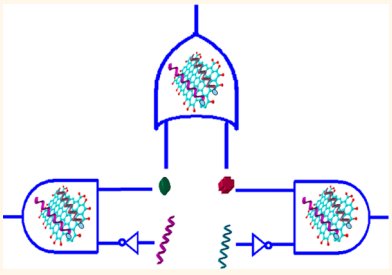

KEYWORDS: logic gates · graphene · aptamer · multiplex detection · ATP · thrombin

DNA logic gates with Boolean functions have been realized by means of DNA and are able to process information and perform arithmetic operations.[1−4] Because of the molecular recognition ability of DNA, DNA logic gates have found applications in biosensing and diagnostics.[5−8] A key to realize the DNA logic-gate-based biosensing is that logic gates can respond smartly to analyte at very low concentration so that a sensitive biosensor can be fabricated. Although encouraging progress has been made in this field, to make simple, sensitive, and selective DNA logic-gate-based biosensors is still a great challenge. Aptamers are artificially selected functional DNA or RNA oligonucleotides that possess highly specific and precise molecular recognition capabilities that can be evolved through genetic engineering.[9−12] Aptamers exhibit many unprecedented advantages compared with antibodies or other biomimetic receptors: aptamers can be selected to bind essentially any molecule of choice, have comparable or even better target affinity, easy and cost-effective synthesis with high reproducibility and purity, and simple and straightforward chemical modification.[13−17] Thus, aptamers can be considered as a potential alternative to antibodies or other biomimetic receptors for the development of biotechnology, diagnostics, and therapy.[18−24] For the DNA logic gates, *in vitro*-selected aptamers present an opportunity to design these logic gates which can exploit any target molecule of choice as an input chemical.[21,25]

Graphene is a one-atom-thick 2D nanomaterial with extraordinary electronic, thermal, and mechanical properties.[26−30] Graphene, along with graphene oxide (GO), could serve as good support for biomolecules due to its large surface area (theoretical limitation: 2630 $m^2 g^{-1}$), flat surface, and rich π-conjugation structure.[31−33] GO could bind and quench a dye-labeled single-stranded DNA probe. In the case of the target present, the specific binding between the dye-labeled probe with its target molecule occurs, which alters the conformation of the probe, disturbs the interaction between the probe and GO, and restores the fluorescence of the dye, and the specific GO/DNA interaction has found important application in the development of biosensing.[18,34−36]

In this work, by taking advantage of the unique GO/aptamer interaction and high binding specificity of aptamers, we developed a new platform to construct logic gates (OR and INHIBIT logic gates) whose states could be controlled in response to complex chemical environments. 6-Carboxyfluorescein (FAM)-labeled adenosine

* Address correspondence to ekwang@ciac.jl.cn, dongsj@ciac.jl.cn.

Received for review March 6, 2012 and accepted July 23, 2012.

Published online July 23, 2012
10.1021/nn300997f

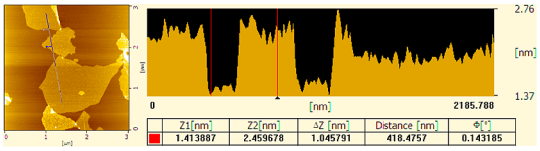

Figure 1. AFM image of GO sheets deposited on a mica substrate.

triphosphate binding aptamer (ABA) and FAM-labeled thrombin binding aptamer (TBA) were first adsorbed onto GO to form a GO/ABA/TBA complex, leading to the quenching of the fluorescence of FAM. In the presence of adenosine triphosphate (ATP) or thrombin, the fluorescence was recovered when ABA or TBA formed a duplex with its target, and the OR logic gate operation could be built by using the restored fluorescence as the reporter for signal output. When ATP and its FAM-free binding aptamer served as two inputs, INHIBIT logic gate was realized by using the induced fluorescence signal as output. Another INHIBIT logic gate in the similar way as the previous INHIBIT logic gate was also realized by using thrombin and its FAM-free binding aptamer as inputs. Meanwhile, the integration of OR and INHIBIT logic gates provided an interesting approach for logic sensing applications where multiple target molecules were present. This proof of concept might provide a new approach for multiplex analysis and nanobiomedical devices responding to multiple input chemicals.

RESULTS AND DISCUSSION

Well-dispersed GO, prepared according to the literature,[37] was used throughout the experiments. As shown in Figure 1, atomic force microscopy (AFM) study reveals that the thickness of GO is about 1.05 nm, characteristic of a fully exfoliated GO sheet.[38] GO is functionalized with negatively charged oxygen moieties. The oxygen/carbon atomic ratio (O/C) of GO is 38% (from XPS data), and there are still many π-conjugated domains present on GO. Also, GO has a high specific surface area. These afford the good loading capacity of GO for ssDNA *via* $\pi-\pi$ interaction.

The principle of the GO/aptamer system to perform an OR logic gate was schemed in Figure 2A. FAM-labeled ATP binding aptamer (ABA, 5′-FAM-ACCTGG-GGGAGTATTGCGGAGGAAGGT-3′ (FAM = 6-carboxy-fluorescein)) and thrombin binding aptamer (TBA, 5′-FAM-AGTCCGTGGTAGGGCAGGTTGGGGTGACT-3′) were utilized as our models. ABA and TBA were first mixed with GO solution to form the GO/ABA/TBA complex, in which the fluorescence of FAM was quenched *via* energy transfer from FAM to GO (Figure S1, Supporting Information). Figure 2B shows the fluorescence spectra of the GO/ABA/TBA complex at different conditions. When neither ATP nor thrombin was present, there was almost no fluorescence due to the strong adsorption of the aptamers on GO and the high

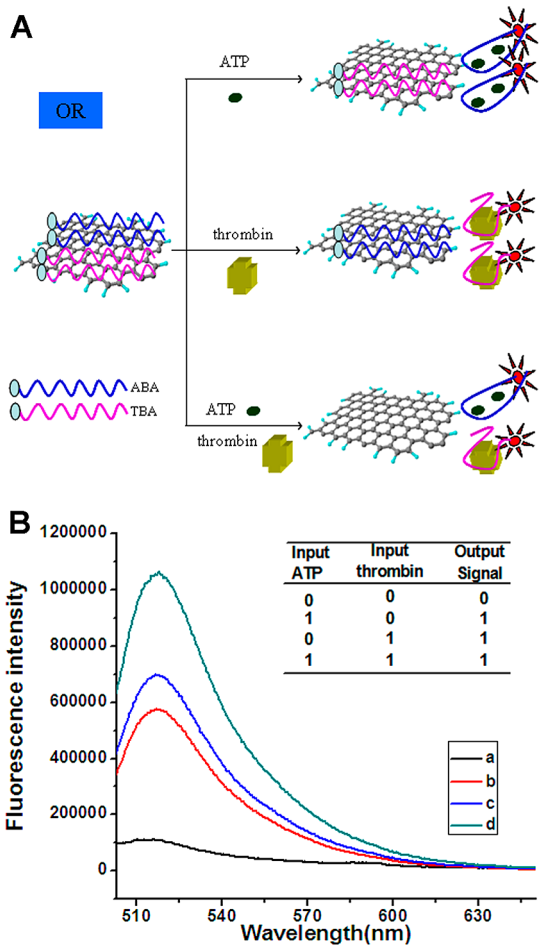

Figure 2. (A) Schematic representation of the OR logic gate. (B) Fluorescence emission of the OR logic gate. (a) GO/ABA/TBA complex; (b) GO/ABA/TBA complex treated with ATP (2 mM); (c) GO/ABA/TBA complex treated with thrombin (30 nM); (d) GO/ABA/TBA complex treated with ATP (2 mM) and thrombin (30 nM). The inset of panel B is the truth table of the OR logic gate.

fluorescence quenching efficiency of GO. However, upon addition of ATP or thrombin, the GO/ABA/TBA complex had significant fluorescence enhancement due to the specific ABA–ATP recognition or TBA–thrombin recognition, respectively. In the presence of both ATP and thrombin, the signal resulted from ABA–ATP recognition and TBA–thrombin recognition; therefore, higher fluorescence was obtained. The restoring of the fluorescence of the GO/ABA/TBA complex by ATP or thrombin could be used to develop an OR logic gate. We defined a fluorescence intensity of 130 000 as the threshold value. Fluorescence intensities higher and lower than 130 000 were defined as output 1 and output 0, respectively. The truth table of the resulting "OR" logic gate is given in the inset of Figure 2B.

Aptamers have high binding specificity, and our results show that the GO/ABA/TBA complex maintained this advantage. As shown in Figure S2 (Supporting Information), when tested with bovine serum

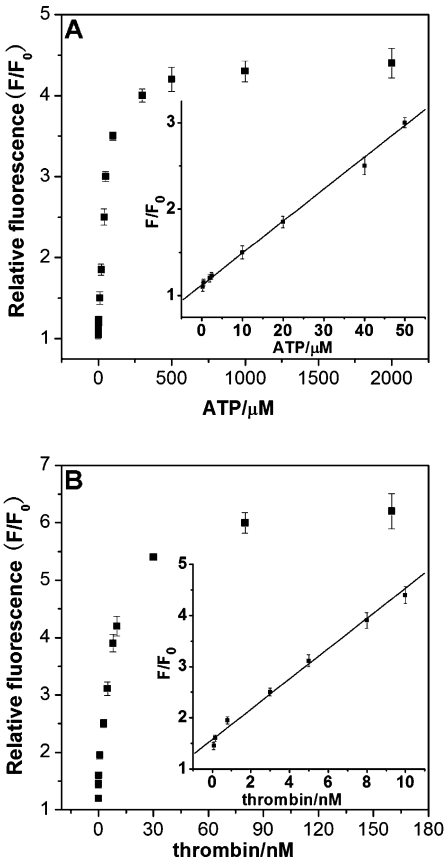

Figure 3. (A) Relative fluorescence changes of GO/ABA/TBA complex *via* the concentrations of ATP. (B) Relative fluorescence changes of GO/ABA/TBA complex *via* the concentrations of thrombin. F_0 and F are the fluorescence intensity without and with the target, respectively.

albumin (BSA), lysozyme, cytidine triphosphate (CTP), thymidine triphosphate (TTP), and guanosine triphosphate (GTP), the GO/ABA/TBA complex exhibits a much lower fluorescence. Figure 3A,B illustrates the fluorescence intensity changes (F/F_0) of the GO/ABA/TBA complex upon addition of different concentrations of ATP and thrombin, respectively. By analyzing the change of fluorescence with the concentrations of ATP, we obtain a linear relationship between the fluorescence and the concentrations of ATP over a range of 500 nM to 50 μM (inset of Figure 3A) and a linear relationship between the fluorescence and the concentrations of thrombin over a range of 0.04−10 nM (inset of Figure 3B). The detection limits of ATP and thrombin are 500 and 0.04 nM, respectively, which can be compared with most existent aptasensors for ATP and thrombin detection.[39−47] The binding affinity between TBA and thrombin is much higher than that between ABA and ATP, K_d(thrombin) = 0.5 nM and K_d(ATP) = 6 ± 3 μM.[48,49] Such a large difference (10^4 times) in K_d might result in 10^4-fold difference in signal sensitivities toward thrombin and ATP in their detections. Circular dichroism (CD) measurements were utilized to monitor the conformation change of

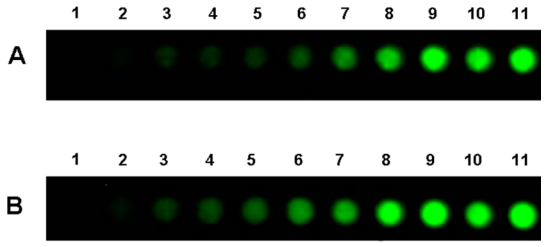

Figure 4. (A) Fluorescence images for the detection of different concentrations of ATP. The concentration of ATP from 1 to 11 is 0, 1, 2, 5, 10, 20, 50, 100, 500, 1000, and 2000 μM, respectively. (B) Fluorescence images for the detection of different concentrations of thrombin. The concentration of thrombin from 1 to 11 is 0, 0.1, 0.2, 0.5, 2, 5, 10, 20, 50, 100, and 200 nM, respectively.

the GO/ABA/TBA complex during the binding events; as shown in Figure S3 (Supporting Information), the formation of quadruplex structures of ABA and TBA was induced by ATP and thrombin, respectively.

Fluorescence intensity of 130 000 was defined as the threshold value, which was dependent on the fluorescence signal corresponding to the detection limits of the two targets, and the fluorescence intensity higher or lower than 130 000 was defined as output 1 or 0, respectively. On the basis of the above definition and the restored fluorescence intensities of the GO/ABA/TBA complex in the presence of a wide range of inputs, the truth table for digital logic was obvious in a certain range of target molecules. Output was 1 in the presence of ATP (≥2 μM) or thrombin (≥0.04 nM). When neither ATP (≥2 μM) nor thrombin (≥0.04 nM) was present, the output was 0. The threshold value corresponded to the fluorescence signal of 2 μM ATP (or 0.04 nM thrombin), which was in the linear range of the sensor (insets of Figure 3). Certainly, the inputs "1" and "0" for ATP and thrombin were also precisely defined. Two micromolar was the boundary between input 1 and 0 for ATP (0.04 nM was the boundary between input 1 and 0 for thrombin). For example, 0 in the input columns of thrombin means it was absent or its concentration was under 0.04 nM. Also, this feature led to the fact that the GO/aptamer systems could be used for the sensitive biosensing (Figure 3) and the following high-throughput analysis of samples (Figure 4). This has obvious advantages, compared to DNA logic systems which use chemicals without biosensing relevance or use high concentrations of chemical as inputs.

The GO/ABA/TBA complex was also applied for high-throughput analysis of ATP and thrombin. The fluorescence images of the assays with different concentrations of ATP are given in Figure 4A, from which the color change is evident with the concentration variation of ATP. With the increase of the concentration of ATP, the fluorescence intensity is enhanced. The fluorescence begins to saturate when the concentration of ATP is above 500 μM. Figure 4B gives the fluorescence screen with different levels of thrombin; with the

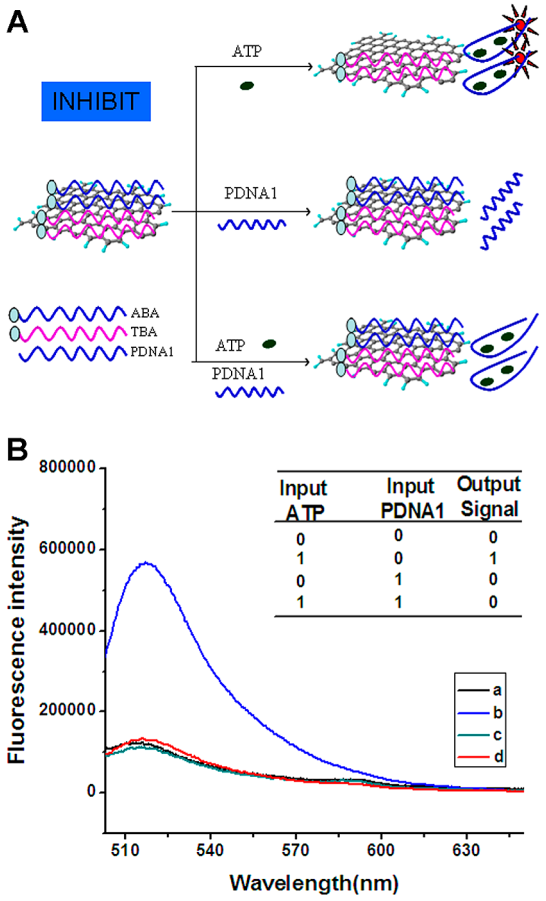

Figure 5. (A) Schematic representation of the INHIBT logic gate based on GO/ABA/TBA complex. (B) Fluorescence emission of the INHIBT logic gate. (a) GO/ABA/TBA complex; (b) GO/ABA/TBA complex treated with ATP (500 μM); (c) GO/ABA/TBA complex treated with PDNA1 (300 μM); (d) GO/ABA/TBA complex treated with ATP (500 μM) and PDNA1 (300 μM). The inset of panel B is the truth table of the INHIBT logic gate.

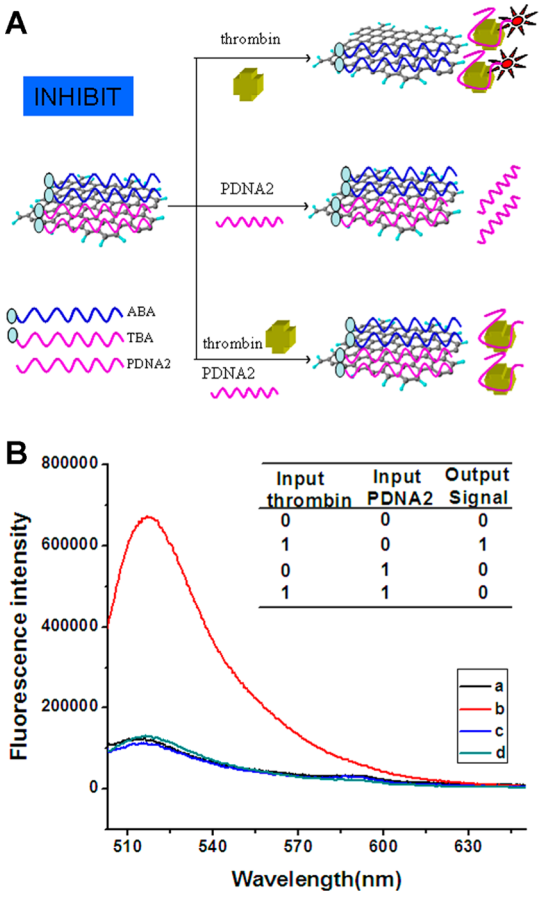

Figure 6. (A) Schematic representation of the INHIBT logic gate based on GO/ABA/TBA complex. (B) Fluorescence emission of the INHIBT logic gate. (a) GO/ABA/TBA complex; (b) GO/ABA/TBA complex treated with thrombin (30 nM); (c) GO/ABA/TBA treated with PDNA2 (30 nM); (d) GO/ABA/TBA complex treated with thrombin (30 nM) and PDNA2 (30 nM). The inset of panel B is the truth table of the INHIBT logic gate.

increase of the concentration of thrombin, the fluorescence intensity is increased and the fluorescence begins to saturate when the concentration of thrombin is above 20 nM. In addition, the used GO/ABA/TBA system in aqueous solution was heated and then centrifuged to separate ATP and thrombin from the solution. After that, ABA and TBA were added to the solution to form the GO/ABA/TBA complex, which could be used for the detecting ATP and thrombin again (Figure S4, Supporting Information).

The OR logic gate is also a potential sensor for the detection of multiple analytes because it can respond to several inputs at the same time. However, it is difficult to figure out which analyte induces the signal. To promote the application of the GO/aptamer system in complex bioanalysis, we designed two INHIBIT logic gates based on the GO/ABA/TBA complex to construct a new sensing platform.

First, we realized the INHIBIT logic gate for ATP using ATP and its FAM-free aptamer (PDNA1) as inputs, which is expressed in Figure 5A. FAM-labeled ABA and TBA were first mixed with GO solution to form a GO/ABA/TBA complex, in which the fluorescence of FAM was quenched. In case desorption of dye-labeled ssDNA from GO occurs, the fluorescence of the dye will be recovered.[31,35] Figure 5B shows the fluorescence emission spectra of the GO/ABA/TBA complex at different conditions. The GO/ABA/TBA complex had significant fluorescence enhancement upon addition of ATP. The fluorescence of the GO/ABA/TBA complex was scarcely influenced by the addition of PDNA1 (CD spectra indicated that PDNA1 could be not adsorbed on the GO/ABA/TBA complex, Figure S5B, Supporting Information). However, when the mixture of ATP and PDNA1 was added, the fluorescence was almost not influenced because PDNA1 bound with two ATP molecules to form a stable helix and successfully suppressed the ATP-induced fluorescence recovery of FAM, indicating that PDNA1 prevented the desorption of ABA from GO. The results were in accord with the truth table of the INHIBIT logic gate.

Subsequently, we designed another INHIBIT logic gate for thrombin in the similar way as the previous

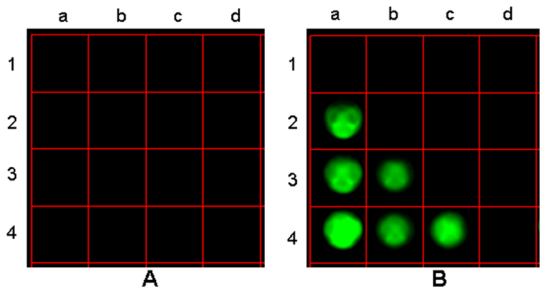

Figure 7. Fluorescence images of GO/ABA/TBA systems before (A) and after reacted with four samples according to the input order in Table 1 (B). Sample 1, no target; sample 2, 100 μM ATP; sample 3, 100 nM thrombin; sample 4, both 100 μM ATP and 100 nM thrombin. The red lines on the images were added in order to distinguish different sample cells.

TABLE 1. Truth Table of Combinatorial Logic Gates for the Detection of ATP and Thrombin in the Samples[a]

	sample	1	1	1	1	
input	PDNA1	0	1	0	1	diagnosis
	PDNA2	0	0	1	1	
output		0	\	\	\	no target
		1	0	\	\	contain ATP
		1	1	0	\	contain thrombin
		1	1	1	0	contain ATP and thrombin

[a] The diagnosis is limited to a certain concentration range. "no target": neither ATP ($\geq$3 μM) nor thrombin ($\geq$0.1 nM) was present; "contain ATP": ATP ($\geq$3 μM) but not thrombin ($\geq$0.1 nM) was present; "contain thrombin": thrombin ($\geq$0.1 nM) but not ATP ($\geq$3 μM) was present; "contain ATP and thrombin": both ATP ($\geq$3 μM) and thrombin ($\geq$0.1 nM) were present. The "\" symbol means that the corresponding condition can be omitted.

INHIBIT logic gate (shown in Figure 6A) by using thrombin and its FAM-free aptamer (PDNA2) as inputs. Figure 6B shows the fluorescence emission spectra of the GO/ABA/TBA complex at different conditions. The fluorescence of FAM-labeled TBA was restored after the addition of thrombin, which bound with the FAM-labeled TBA and induced the recovery of the fluorescence of FAM. The fluorescence of the GO/ABA/TBA complex was not influenced by the addition of PDNA2 (CD spectra indicated that PDNA2 could not be adsorbed on GO/ABA/TBA complex, Figure S5B, Supporting Information). When the mixture of PDNA2 and thrombin was added, the quenched fluorescence was stable because PDNA2 bound with thrombin strongly and successfully inhibited the thrombin-induced fluorescence recovery of FAM. The results were also in accord with the truth table of the INHIBIT logic gate (Figure 6B, inset).

The combinatorial logic gates (OR and INHIBIT) were used to make high-throughput judgment about what targets were present in the input samples (Figure 7 and Figure S6) according to the output results, and the logic operations and diagnosis are summarized in Table 1. The green fluorescence observed was defined as output "1". On the basis of the outputs, we could logically make judgment whether ATP ($\geq$3 μM) or thrombin ($\geq$0.1 nM) was present or not.

As shown in Figure 7, we input sample 1 to a1 cell to interact with the GO/ABA/TBA complex (input 100, in the first column in Table 1) like the condition in the OR logic gate. There was no fluorescence observed (output 0), so we could draw a conclusion that there was "no target" (neither ATP ($\geq$3 μM) nor thrombin ($\geq$0.1 nM) was present), and we did not need to do other tests (the symbol "\" was used to represent these conditions in Table 1). When we input sample 2 to a2 cell (input 100, in the first column in Table 1), the fluorescence was high (output 1). We had to figure out which target was present in sample 2 to induce the restoration of fluorescence. The INHIBT logic gate could help us at this time. We input PDNA1 and sample 2 simultaneously into the system (input 110, in the second column in Table 1). The fluorescence was low (output 0) because the input ATP was blocked by the other input PDNA1 like the condition in the INHIBIT logic gate, which meant sample 2 contained ATP ($\geq$3 μM) but not thrombin ($\geq$0.1 nM). Other tests could be neglected. For sample 3, when we added sample 3 to a3, b3, and c3 cells, a3 and b3 cells showed high fluorescence (output 1), while c3 cell in which PDNA2 and sample 3 were simultaneously input (input 101 in the third column in Table 1) showed low fluorescence (output 0); this meant that it was thrombin ($\geq$0.1 nM) which caused the high fluorescence in the input state 100 and 110, and no ATP ($\geq$3 μM) was contained. For sample 4, when we added sample 4 to a4, b4, c4, and d4 cells, high fluorescence was observed in a4, b4, and c4 cells, but d4 cell gave out a low fluorescence (input 111 in the fourth column in Table 1, output 0) because the two targets were blocked by their aptamers, respectively. We could be sure both ATP ($\geq$3 μM) and thrombin ($\geq$0.1 nM) were in sample 4. We have to pay attention that when the output is diagnosed as "0", two conditions, the target is absent or under its detection limit, are both possible. Upon the above analysis, we can see that high-throughput fluorescence imaging systems based on combinatorial logic gates are powerful for the detection of multiple analytes. We could analyze samples with different targets at the same time as long as we have enough aptamers and diagnose the samples with the help of combinatorial logic gates. The concept may find important applications in DNA logic, biosensors, and bioimaging. Besides aptamers, other functional DNA, such as DNAzyme, RNA aptamer, or motif that might be used to realize similar regulations, deserves to be researched in the future.

CONCLUSIONS

We have demonstrated that the GO/aptamer system could be programmed to perform relatively complicated OR and INHIBIT logic gates by taking advantage

of the unique GO/aptamer interaction and the specific aptamer−target recognition. Multiple targets regulated the fluorescence intensities, and OR and INHIBIT logic gates were operated by the different fluorescence intensities at the same wavelength upon different inputs and then combined to be the combinatorial logic gates. The combinatorial logic gates enabled high-throughput diagnosis by using fluorescence imaging. On the basis of the outputs of the combinatorial logic gates, we could figure out whether ATP ($\geq$3 μM) or thrombin ($\geq$0.1 nM) was present or not. This proof of concept might provide a new approach for multiplex analysis and also a connection between the GO/aptamer interaction, the molecular recognition abilities of aptamers, the design of molecular mimics of logic elements, and the multiplex biosensing. Because aptamers can be selected to bind theoretically any molecule of choice, logic gates based on the GO/aptamer system might be used for detecting other anaytes by using the corresponding aptamers.

EXPERIMENTAL SECTION

Materials. Graphene oxide (GO) was synthesized from natural graphite powder by a modified Hummers method.[37] ABA: 5′ FAM-ACCTGGGGGAGTATTGCGGAGGAAGGT-3′; TBA: 5′-FAM-AGTCCGTGGTAGGGCAGGTTGGGGTGACT-3′; PDNA1: 5′ ACCTGGGGGAGTATTGCGGAGGAAGGT-3′; PDNA2: 5′ AGTCCGTGGTAGGGCAGGTTGGGGTGACT-3′. DNA oligonucleotides were synthesized by Shanghai Sangon Biotechnology Co. DNA oligonucleotide stock solutions were prepared with Tris-HCl buffer (25 mM Tris-HCl, 140 mM NaCl, 5 mM KCl, pH 7.0) and kept frozen. Bovine serum albumin (BSA), lysozyme, adenosine triphosphate (ATP), thrombin, cytidine triphosphate (CTP), thymidine triphosphate (TTP), and guanosine triphosphate (GTP), purchased from Sigma, were prepared in the Tris-HCl buffer (20 mM Tris-HCl, 140 mM NaCl, 5 mM KCl, pH 7.4). Graphite powder was purchased from China National Pharmaceutical Group Corporation (Shanghai, China). All other chemicals not mentioned here were of analytical reagent grade and used as received. Double distilled water was used throughout.

Instruments. Fluorescence measurements were carried out on a Fluoromax-4 spectrofluorometer (Horiba Jobin Yvon Inc., France). The unit of the fluorescence signal is cps (counts per second). The light source is a 150 W ozone-free xenon lamp. The emission spectra were recorded in the wavelength range of 500−650 nm upon excitation at 492 nm. Excitation and emission slits were set at 5 and 5 nm, respectively. Increment of 1.0 nm and integration time of 0.1 s were used. Then the fluorescence was also imaged by Maestro 500FL *in vivo* imaging system from Cambridge Research & Instrumentation, Inc. (CRI), USA. The imaging system used in this study consisted of a light-tight box equipped with a 150 W halogen lamp and an excitation filter system (500−555 nm) to excite FAM. Fluorescence was detected by a CCD camera equipped with a C-mount lens and an emission filter (580 nm long pass). The resulting data can be used to identify, separate, and remove the contribution of autofluorescence in analyzed images by a commercial software (MaestroTM 2.4). For the comparison between different targets, a microtiter plate was put on a nonfluorescent board; they were imaged under the same excitation conditions. AFM was performed on a SPI3800N microscope instrument (Seiko Instruments, Inc., Japan) in tapping-mode in air at ambient temperature. CD spectra were collected by a JASCO J-810 spectropolarimeter (Tokyo, Japan), of which the lamp was always kept under a stable stream of dry purified nitrogen (99.99%) during experiments. Three scans from 210 to 350 at 0.1 nm intervals were accumulated and averaged.

OR Logic Gate Based on GO/ABA/TBA Complex. Preparation of GO/ABA/TBA complex: GO solution (20 μg/mL), ABA (50 nM), and TBA (50 nM) were mixed for 10 min at room temperature to form the GO/ABA/TBA complex. As shown in Figure S1, the fluorescence of ABA and TBA was quenched by GO.

Four Eppendorf tubes each contained 400 μL of the GO/ABA/TBA complex and then were mixed with the four possible input combinations for 30 min (30 min was enough to reach the maximum fluorescence, as shown in Figure S7): (00) 400 μL of Tris-HCl buffer; (10) 400 μL of ATP (2 mM); (01) 400 μL of thrombin (30 nM); (11) 200 μL of ATP (2 mM) and 200 μL of thrombin (30 nM). The contents of each tube were then analyzed individually by excitation at 492 nm and recording the fluorescence emission at 520 nm.

OR logic gate for the detection of ATP and thrombin: 400 μL of GO/ABA/TBA complex was mixed with 400 μL of different concentrations of ATP or thrombin, reacted for 0.5 h, then the fluorescence spectra were recorded.

First INHIBIT Logic Gate Based on GO/ABA/TBA Complex. The principle of INHIBIT logic gate based on GO/ABA/TBA complex was schemed in Figure 5A. Four Eppendorf tubes each contained 400 μL of the GO/ABA/TBA complex and then were mixed with the four possible input combinations for 30 min (30 min was enough to reach the maximum fluorescence, as shown in Figure S8), then recorded the fluorescence spectra: (00) 400 μL of Tris-HCl buffer; (10) 400 μL of ATP (500 μM); (01) 400 μL of PDNA1 (300 μM); (11) 200 μL of ATP (500 μM) and 200 μL of PDNA1 (300 μM). The contents of each tube were then analyzed individually by excitation at 492 nm and recording the fluorescence emission at 520 nm.

Second INHIBIT Logic Gate Based on GO/ABA/TBA Complex. The principle of INHIBIT logic gate based on GO/ABA/TBA complex was schemed in Figure 6A. Four Eppendorf tubes each contained 400 μL of the GO/ABA/TBA complex and then were mixed with the four possible input combinations for 30 min before the fluorescence spectra were recorded (Figure S9 shows the time-dependent fluorescence changes for the INHIBIT logic gate upon four input combinations, 30 min was enough to reach the maximum fluorescence): (00) 400 μL of Tris-HCl buffer; (10) 400 μL of thrombin (30 nM); (01) GO/ABA/TBA complex mixed with 400 μL of PDNA2 (30 nM); (11) GO/ABA/TBA complex mixed with 200 μL of thrombin (30 nM) and 200 μL of PDNA2 (30 nM). The contents of each tube were then analyzed individually by excitation at 492 nm and recording the fluorescence emission at 520 nm.

Conflict of Interest: The authors declare no competing financial interest.

Acknowledgment. This work was supported by the National Natural Science Foundation of China (200935003, 21075116) and 973 projects (2011CB911002, 2010CB933603).

Supporting Information Available: Figures S1−S9. This material is available free of charge *via* the Internet at http://pubs.acs.org.

REFERENCES AND NOTES

1. Adleman, L. M. Molecular Computation of Solutions to Combinatorial Problems. *Science* **1994**, *266*, 1021–1024.
2. Lipton, R. J. DNA Solution of Hard Computational Problems. *Science* **1995**, *268*, 542–545.
3. Pasotti, L.; Quattrocelli, M.; Galli, D.; De Angelis, M. G. C.; Magni, P. Multiplexing and Demultiplexing Logic Functions for Computing Signal Processing Tasks in Synthetic Biology. *Biotechnol. J.* **2011**, *6*, 784–795.
4. Szacilowski, K. Digital Information Processing in Molecular Systems. *Chem. Rev.* **2008**, *108*, 3481–3548.

5. Genot, A. J.; Bath, J.; Turberfield, A. J. Reversible Logic Circuits Made of DNA. *J. Am. Chem. Soc.* **2011**, *133*, 20080–20083.
6. Li, T.; Zhang, L.; Ai, J.; Dong, S.; Wang, E. Ion-Tuned DNA/Ag Fluorescent Nanoclusters as Versatile Logic Device. *ACS Nano* **2011**, *5*, 6334–6338.
7. Wu, Z.; Tang, L. J.; Zhang, X. B.; Jiang, J. H.; Tan, W. H. Aptamer-Modified Nanodrug Delivery Systems. *ACS Nano* **2011**, *5*, 7696–7699.
8. Zhu, J.; Li, T.; Zhang, L.; Dong, S.; Wang, E. G-Quadruplex DNAzyme Based Molecular Catalytic Beacon for Label-Free Colorimetric Logic Gates. *Biomaterials* **2011**, *32*, 7318–7324.
9. Ellington, A. D.; Szostak, J. W. *In Vitro* Selection of RNA Molecules That Bind Specific Ligands. *Nature* **1990**, *346*, 818–822.
10. Mascini, M.; Palchetti, I.; Tombelli, S. Nucleic Acid and Peptide Aptamers: Fundamentals and Bioanalytical Aspects. *Angew. Chem., Int. Ed.* **2012**, *51*, 1316–1332.
11. Robertson, D. L.; Joyce, G. F. Selection *in Vitro* of an RNA Enzyme That Specifically Cleaves Single-Stranded-DNA. *Nature* **1990**, *344*, 467–468.
12. Tuerk, C.; Gold, L. Systematic Evolution of Ligands by Exponential Enrichment - RNA Ligands to Bacteriophage-T4 DNA-Polymerase. *Science* **1990**, *249*, 505–510.
13. Bagalkot, V.; Gao, X. SiRNA-Aptamer Chimeras on Nanoparticles: Preserving Targeting Functionality for Effective Gene Silencing. *ACS Nano* **2011**, *5*, 8131–8139.
14. Centi, S.; Tombelli, S.; Minunni, M.; Mascini, M. Aptamer-Based Detection of Plasma Proteins by an Electrochemical Assay Coupled to Magnetic Beads. *Anal. Chem.* **2007**, *79*, 1466–1473.
15. Wu, Y.; Sefah, K.; Liu, H.; Wang, R.; Tan, W. DNA Aptamer-Micelle as an Efficient Detection/Delivery Vehicle toward Cancer Cells. *Proc. Natl. Acad. Sci. U.S.A.* **2010**, *107*, 5–10.
16. Xiang, Y.; Tong, A.; Lu, Y. Abasic Site-Containing DNAzyme and Aptamer for Label-Free Fluorescent Detection of Pb^{2+} and Adenosine with High Sensitivity, Selectivity, and Tunable Dynamic Range. *J. Am. Chem. Soc.* **2009**, *131*, 15352–15357.
17. Zhao, Q.; Li, X. F.; Shao, Y.; Le, X. C. Aptamer-Based Affinity Chromatographic Assays for Thrombin. *Anal. Chem.* **2008**, *80*, 7586–7593.
18. Gulbakan, B.; Yasun, E.; Shukoor, M. I.; Zhu, Z.; You, M.; Tan, X.; Sanchez, H.; Powell, D. H.; Dai, H.; Tan, W. A Dual Platform for Selective Analyte Enrichment and Ionization in Mass Spectrometry Using Aptamer-Conjugated Graphene Oxide. *J. Am. Chem. Soc.* **2010**, *132*, 17408–17410.
19. Hamula, C. L. A.; Zhang, H. Q.; Li, F.; Wang, Z. X.; Le, X. C.; Li, X. F. Selection and Analytical Applications of Aptamers Binding Microbial Pathogens. *TrAC, Trends Anal. Chem.* **2011**, *30*, 1587–1597.
20. Li, F.; Li, J. J.; Wang, C. A.; Zhang, J.; Li, X. F.; Le, X. C. Competitive Protection of Aptamer-Functionalized Gold Nanoparticles by Controlling the DNA Assembly. *Anal. Chem.* **2011**, *83*, 6464–6467.
21. Liu, J. W.; Lu, Y. Smart Nanomaterials Responsive to Multiple Chemical Stimuli with Controllable Cooperativity. *Adv. Mater.* **2006**, *18*, 1667–1671.
22. Nielsen, L. J.; Olsen, L. F.; Ozalp, V. C. Aptamers Embedded in Polyacrylamide Nanoparticles: A Tool for *In Vivo* Metabolite Sensing. *ACS Nano* **2010**, *4*, 4361–4370.
23. Pang, Y. F.; Xu, Z. A.; Sato, Y.; Nishizawa, S.; Teramae, N. Base Pairing at the Abasic Site in DNA Duplexes and Its Application in Adenosine Aptasensors. *ChemBioChem* **2012**, *13*, 436–442.
24. Scarano, S.; Ermini, M. L.; Spirit, M. M.; Mascini, M.; Bogani, P.; Minunni, M. Simultaneous Detection of Transgenic DNA by Surface Plasmon Resonance Imaging with Potential Application to Gene Doping Detection. *Anal. Chem.* **2011**, *83*, 6245–6253.
25. Xu, X. W.; Zhang, J.; Yang, F.; Yang, X. R. Colorimetric Logic Gates for Small Molecules Using Split/Integrated Aptamers and Unmodified Gold Nanoparticles. *Chem. Commun.* **2011**, *47*, 9435–9437.
26. Geim, A. K.; Novoselov, K. S. The Rise of Graphene. *Nat. Mater.* **2007**, *6*, 183–191.
27. Kotov, N. A. Materials Science: Carbon Sheet Solutions. *Nature* **2006**, *442*, 254–255.
28. Lee, C.; Wei, X. D.; Kysar, J. W.; Hone, J. Measurement of the Elastic Properties and Intrinsic Strength of Monolayer Graphene. *Science* **2008**, *321*, 385–388.
29. Novoselov, K. S.; Geim, A. K.; Morozov, S. V.; Jiang, D.; Zhang, Y.; Dubonos, S. V.; Grigorieva, I. V.; Firsov, A. A. Electric Field Effect in Atomically Thin Carbon Films. *Science* **2004**, *306*, 666–669.
30. Service, R. F. Graphene Recipe Yields Carbon Cornucopia. *Science* **2008**, *322*, 1785–1785.
31. He, S. J.; Song, B.; Li, D.; Zhu, C. F.; Qi, W. P.; Wen, Y. Q.; Wang, L. H.; Song, S. P.; Fang, H. P.; Fan, C. H. A Graphene Nanoprobe for Rapid, Sensitive, and Multicolor Fluorescent DNA Analysis. *Adv. Funct. Mater.* **2009**, *19*, 1–7.
32. Guo, C. X.; Zheng, X. T.; Lu, Z. S.; Lou, X. W.; Li, C. M. Biointerface by Cell Growth on Layered Graphene-Artificial Peroxidase-Protein Nanostructure for *In Situ* Quantitative Molecular Detection. *Adv. Mater.* **2010**, *22*, 5164–5167.
33. Wen, Y. Q.; Xing, F. F.; He, S. J.; Song, S. P.; Wang, L. H.; Long, Y. T.; Li, D.; Fan, C. H. A Graphene-Based Fluorescent Nanoprobe for Silver(I) Ions Detection by Using Graphene Oxide and a Silver-Specific Oligonucleotide. *Chem. Commun.* **2010**, *46*, 2596–2598.
34. Bonanni, A.; Pumera, M. Graphene Platform for Hairpin-DNA-Based Impedimetric Genosensing. *ACS Nano* **2011**, *5*, 2356–2361.
35. Lu, C. H.; Yang, H. H.; Zhu, C. L.; Chen, X.; Chen, G. N. A Graphene Platform for Sensing Biomolecules. *Angew. Chem., Int. Ed.* **2009**, *48*, 4785–4787.
36. Wang, Y.; Li, Z. H.; Hu, D. H.; Lin, C. T.; Li, J. H.; Lin, Y. H. Aptamer/Graphene Oxide Nanocomplex for *in Situ* Molecular Probing in Living Cells. *J. Am. Chem. Soc.* **2010**, *132*, 9274–9276.
37. Hummers, W. S.; Offeman, R. E. Preparation of Graphitic Oxide. *J. Am. Chem. Soc.* **1958**, *80*, 1339–1339.
38. Li, D.; Muller, M. B.; Gilje, S.; Kaner, R. B.; Wallace, G. G. Processable Aqueous Dispersions of Graphene Nanosheets. *Nat. Nanotechnol.* **2008**, *3*, 101–105.
39. Du, Y.; Li, B. L.; Wei, H.; Wang, Y. L.; Wang, E. K. Multifunctional Label-Free Electrochemical Biosensor Based on an Integrated Aptamer. *Anal. Chem.* **2008**, *80*, 5110–5117.
40. Lu, Y.; Li, X. C.; Zhang, L. M.; Yu, P.; Su, L.; Mao, L. Q. Aptamer-Based Electrochemical Sensors with Aptamer-Complementary DNA Oligonucleotides as Probe. *Anal. Chem.* **2008**, *80*, 1883–1890.
41. Zuo, X. L.; Song, S. P.; Zhang, J.; Pan, D.; Wang, L. H.; Fan, C. H. A Target-Responsive Electrochemical Aptamer Switch (TREAS) for Reagentless Detection of Nanomolar ATP. *J. Am. Chem. Soc.* **2007**, *129*, 1042–1043.
42. Ding, J. W.; Chen, Y.; Wang, X. W.; Qin, W. Label-Free and Substrate-Free Potentiometric Aptasensing Using Polycation-Sensitive Membrane Electrodes. *Anal. Chem.* **2012**, *84*, 2055–2061.
43. Liu, X. Q.; Freeman, R.; Golub, E.; Willner., I. Chemiluminescence and Chemiluminescence Resonance Energy Transfer (CRET) Aptamer Sensors Using Catalytic Hemin/G-Quadruplexes. *ACS Nano* **2011**, *5*, 7648–7655.
44. Rotem, D.; Jayasinghe, L.; Salichou, M.; Bayley, H. Protein Detection by Nanopores Equipped with Aptamers. *J. Am. Chem. Soc.* **2012**, *134*, 2781–2787.
45. Wang, Y. Y.; Liu, B. Conjugated Polyelectrolyte-Sensitized Fluorescent Detection of Thrombin in Blood Serum Using Aptamer-Immobilized Silica Nanoparticles as the Platform. *Langmuir* **2009**, *25*, 12787–12793.
46. Tennico, Y. H.; Hutanu, D.; Koesdjojo, M. T.; Bartel, C. M.; Remcho, V. T. On-Chip Aptamer-Based Sandwich Assay for Thrombin Detection Employing Magnetic Beads and Quantum Dots. *Anal. Chem.* **2010**, *82*, 5591–5597.

47. Chang, H. X.; Tang, L. H.; Wang, Y.; Jiang, J. H.; Li, J. H. Graphene Fluorescence Resonance Energy Transfer Aptasensor for the Thrombin Detection. *Anal. Chem.* **2010**, *82*, 2341–2346.
48. Zhou, G. P.; Huang, X. R.; Qu, Y. Q. The Binding Effect of Aptamers on Thrombin. *Biochem. Eng. J.* **2010**, *52*, 117–122.
49. Huizenga, D. E.; Szostak, J. W. A DNA Aptamer That Binds Adenosine and ATP. *Biochemistry* **1995**, *34*, 656–665.